REGULAR ARTICLE

WILEY

Development of a sweet pepper harvesting robot

Boaz Arad[1] | Jos Balendonck[2] | Ruud Barth[2] | Ohad Ben-Shahar[1] |
Yael Edan[3] | Thomas Hellström[4] | Jochen Hemming[2] | Polina Kurtser[3] |
Ola Ringdahl[4] | Toon Tielen[2] | Bart van Tuijl[2]

[1]Department of Computer Science, Ben-Gurion University of the Negev, Beer-Sheva, Israel

[2]Greenhouse Horticulture, Wageningen University & Research, Wageningen, The Netherlands

[3]Department of Industrial Engineering and Management, Ben-Gurion University of the Negev, Beer-Sheva, Israel

[4]Department of Computing Science, Umeå University, Umeå, Sweden

Correspondence
Ola Ringdahl, Department of Computing Science, Umeå University, 901 87 Umeå, Sweden.
Email: ringdahl@cs.umu.se

Funding information
Horizon 2020 Framework Program, Grant/Award Number: 644313

Abstract

This paper presents the development, testing and validation of SWEEPER, a robot for harvesting sweet pepper fruit in greenhouses. The robotic system includes a six degrees of freedom industrial arm equipped with a specially designed end effector, RGB-D camera, high-end computer with graphics processing unit, programmable logic controllers, other electronic equipment, and a small container to store harvested fruit. All is mounted on a cart that autonomously drives on pipe rails and concrete floor in the end-user environment. The overall operation of the harvesting robot is described along with details of the algorithms for fruit detection and localization, grasp pose estimation, and motion control. The main contributions of this paper are the integrated system design and its validation and extensive field testing in a commercial greenhouse for different varieties and growing conditions. A total of 262 fruits were involved in a 4-week long testing period. The average cycle time to harvest a fruit was 24 s. Logistics took approximately 50% of this time (7.8 s for discharge of fruit and 4.7 s for platform movements). Laboratory experiments have proven that the cycle time can be reduced to 15 s by running the robot manipulator at a higher speed. The harvest success rates were 61% for the best fit crop conditions and 18% in current crop conditions. This reveals the importance of finding the best fit crop conditions and crop varieties for successful robotic harvesting. The SWEEPER robot is the first sweet pepper harvesting robot to demonstrate this kind of performance in a commercial greenhouse.

KEYWORDS
agriculture, computer vision, field test, motion control, real-world conditions, robotics

1 | INTRODUCTION

In modern greenhouses, there is a high demand to automate labor. The availability of a skilled workforce that accepts repetitive tasks in harsh greenhouse climate conditions is decreasing rapidly. The resulting increase in labour costs and reduced capacity put major pressure on the competitiveness of the greenhouse sector (Comba, Gay, Piccarolo, & Ricauda Aimonino, 2010).

The performance of robots for automated harvesting of fruits and vegetables has remained remarkably stationary in the past three decades. Around 50 robotic harvesting systems have thus far been globally developed, of which none have been successfully commercialized to this date (Bac, van Henten, Hemming, & Edan, 2014). On average, the

harvesting success of prototypes has been around 66% (values ranging between 40% and 86%), with cycle times of 33 s per fruit (values ranging between 1 and 227 s). This performance is far below what is commercially viable, under the assumption that the market demands a machine that is highly accurate and fast. However, near-perfect harvest success and high speed are not necessarily prerequisites for economic viability, and also robots with lower performance can be of supportive value. The major problem is rather the gap between the required and achieved technological readiness level. In particular, earlier presented solutions most often lack practical robustness, failure control, and required postharvest logistics.

The goal of the European Union-funded research project SWEEPER[1] was to develop, test and validate a practical robotic harvesting solution for sweet peppers in real-world conditions.

This paper describes various aspects of the project, from the scientific and technical challenges and solutions to the results of extensive field tests (262 fruits along 4 weeks) in a commercial greenhouse with a large variety of conditions (different growing rows, as well as different fruit varieties/crop conditions). The specific hypotheses tested were whether harvesting performance depend on the sweet pepper variety and crop modifications. Furthermore, the robot was integrated into the logistics of the greenhouse (equipped with a mobile platform which autonomously traversed along the rows).

2 | STATE OF THE ART

Agricultural robots are being developed for many agricultural tasks such as field cultivation, planting, harvesting, pruning, and spraying (Baxter, Cielniak, Hanheide, & From, 2018; Bechar & Vigneault, 2017; Blackmore, 2016; Duckett, Pearson, Blackmore, Grieve, & Smith, 2018; Edan, Han, & Kondo, 2009; van Henten, Bac, Hemming, & Edan, 2013). In practice, current working agricultural robotics systems are limited despite intensive R&D and many feasible technical solutions that have proven successful (Blackmore, 2016; Duckett et al., 2018). Fully robotized operations are not yet available, mostly due to the unstructured, dynamically changing, and undefined agricultural environment that demands a high level of sophistication and complicates the development process (Bac et al., 2014). Furthermore, each crop and task requires tailored designed developments (Bac et al., 2014). However, a number of companies have recently announced that they are close to a commercial product launch. Examples are robots for harvesting strawberries (Agrobot[2], Octinion[3]) and harvesting and deleafing of tomatoes (Priva[4], Panasonic[5]).

Due to the complex problem, most R&D on robotic harvesting focuses on a single aspect of the robotic system, for example, detection (Halstead, McCool, Denman, Perez, & Fookes, 2018; Kamilaris & Prenafeta-Boldú, 2018; Kapach, Barnea, Mairon, Edan, & Ben-Shahar, 2012; Vitzrabin & Edan, 2016a, 2016b; Zemmour, Kurtser, & Edan, 2019; Zhao, Gong, Huang, & Liu, 2016), manipulation and gripping (Bulanon & Kataoka, 2010; Eizicovits & Berman, 2014; Eizicovits, van Tuijl, Berman, & Edan, 2016; Rodríguez, Moreno, Sánchez, & Berenguel, 2013; Tian, Zhou, & Gu, 2018), and motion/task planning (Barth, IJsselmuiden, Hemming, & Van Henten, 2016; Korthals et al., 2018; Kurtser & Edan, 2019; Li & Qi, 2018; Liu, ElGeneidy, Pearson, Huda, & Neumann, 2018; Ringdahl, Kurtser, & Edan, 2019).

Currently reported attempts of fully integrated autonomous harvesting include melon (Edan, Rogozin, Flash, & Miles, 2000), cucumber (van Henten et al., 2002, 2003), strawberry (Hayashi et al., 2010), cherry tomato (Feng, Zou, Fan, Zhang, & Wang, 2018; Tanigaki, Fujiura, Akase, & Imagawa, 2008), eggplant (Hayashi, Ganno, Ishii, & Tanaka, 2002, apple (De-An, Jidong, Wei, Ying, & Yu, 2011; Silwal et al., 2017; Yuan, Lei, Xin, & Bing, 2016), orange (Almendral et al., 2018; Ferreira, Sanchez, Braunbeck, & Santos, 2018), and sweet peppers harvesting (Bac et al., 2017; Lehnert, English, McCool, Tow, & Perez, 2017). However, most research to date has been has been tested either in simulation (Edan & Miles, 1993; Shamshiri et al., 2018; Wang et al., 2018) or in laboratory conditions (Almendral et al., 2018; Ceres, Pons, Jimenez, Martin, & Calderon, 1998; Foglia & Reina, 2006). Very few works have been tested in field conditions (Bac et al., 2017; Bontsema et al., 2014; De-An et al., 2011; Edan & Miles, 1993; Hayashi et al., 2010; van Henten et al., 2003; Lehnert et al., 2017). Furthermore, these field tests were limited and did not include a wide range of conditions (different seasons, times along the day) and different plants (cultivars, growing conditions). Overall, the number of test samples evaluated in 56 cases reported varied from 11 to 2,506 (Bac et al., 2014). Recent studies that present new developments are still very limited in performance evaluation. For example, the gripper of a sweet pepper harvester tested on an integrated system in a Dutch commercial greenhouse for 176 fruits of single cultivar crops in simplified and unmodified crop along 8 days in the same month. A sweet pepper harvester by another development (Lehnert et al., 2017) was tested in a commercial Australian greenhouse in two field trials with total 50 fruits along 10 m crop. An apple harvester (Silwal et al., 2017) tested in a commercial orchard in Washington State evaluated performance for 150 fruits with no details on how many trees this included and/or timing of the tests. Other agricultural robots tested in field conditions include a pruning robot (Botterill et al., 2017) that was tested on a single row of one cultivar in 1 month and spraying robots (Adamides et al., 2017; Berenstein & Edan, 2018) that were tested in actual vineyard conditions focusing on human–robot interaction evaluation.

Given the complexity of harvesting that is highly variable in the environment and operating conditions (Kurtser & Edan, 2018), it is questionable whether the reliability of a performance indicator

---

[1]Sweeper website http://sweeper-robot.eu. Accessed February 28, 2019.

[2]http://agrobot.com. Accessed on March 17, 2019.

[3]http://octinion.com. Accessed on March 17, 2019.

[4]https://www.priva.com/discover-priva/news-and-stories/priva-kompano-deleaf-line. Accessed March 17, 2019.

[5]https://internetofbusiness.com/panasonic-robot-tomato-picker. Accessed on March 17, 2019.

based on such few fruit samples can represent the robot performance in the complex crop environment (Bac et al., 2014). Moreover, these test samples were probably evaluated at a specific hour on a day and did not include the weather variations throughout the day. Furthermore, even when a full system is tested, it usually does not include the full integration into the crop logistics and details on actual experimental conditions are not always fully reported.
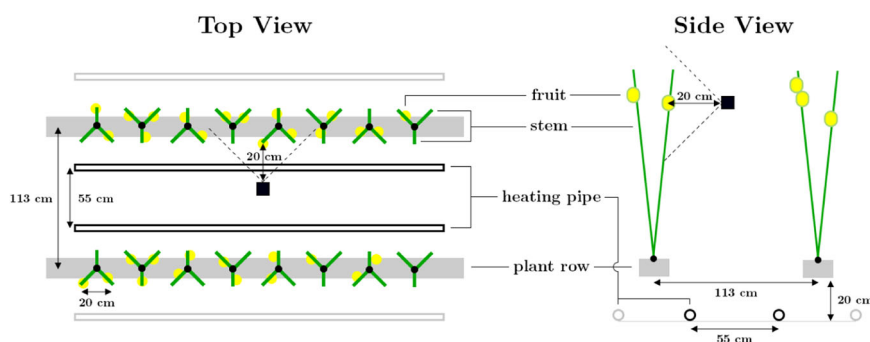
Due to the large variation throughout and between seasons, it is important to conduct long-term tests in a variety of conditions and for different crop varieties (Bac et al., 2014; Edan & Miles, 1994) and mostly report testing conditions.

3 | ENVIRONMENT AND REQUIREMENTS

In Figure 1, a typical growing system of a commercial sweet pepper crop in a modern Dutch greenhouse is illustrated. Figure 2 shows the crop from two different perspectives. The heating pipes form the central infrastructure of the greenhouse on which harvest and crop maintenance carts can move between two rows of plants. Each plant consists of three stems, and the plants are placed to form double plant stem rows (V-system, in the following referred to as the double-row cropping system) with on average 20 cm spacing between stems along the aisle. Plants are positioned on a hanging gutter that is attached to the roof of the greenhouse. Plant stems are guided along a vertical support wire. The average plant stem density is 7.2 stems/m². Conditions in the greenhouse vary a lot during the day (e.g., illumination, temperature) and during the season (e.g., crop reaches a height of 4.5 m toward the end of the season).

The robot was designed to operate in a commercial greenhouse with the following requirements:

- Ability to harvest ripe (yellow colored) fruits in the greenhouse.
- Should not damage the harvested fruit body or fruit stem (peduncle).
- Should not damage other fruits, plants, or guide wires.
- Must interface with automatic guided vehicle logistics.

4 | SYSTEM DESIGN AND OPERATION

On the basis of the requirements outlined in the previous section, an initial robot design was proposed and developed. Field tests of partial solutions called for alternative solutions, which were then developed and tested in an iterative manner. In the remaining part of this section, the final design is described. The overall operation of the robot and algorithms for fruit detection, grasp pose estimation, and motion control are detailed.

4.1 | Overall design

An overview of the robotic system is shown in Figure 3. The system was composed of a standard six degrees of freedom (DOF) industrial robot arm (Fanuc LR Mate 200iD), a custom designed end effector (patent No PCT/NL2019/050396–pending approval), a high-end main computer with graphics processing unit (GPU), programmable logic controllers (PLCs), sensors, other electronic equipment, and a small container to store harvested fruit. One Arduino-based PLC controlled the cart operations (motion along the row and cart elevation); another PLC controlled the low-level functions of the end effector. All equipment was mounted on a cart that could drive on the pipe rail and also on the concrete floor. The cart is a modification of the commercially available Qii-Drive Pepper AGV pepper harvest cart (Bogaerts Greenhouse Logistics, Belgium). This cart has a scissor lift that can elevate the platform with the robot manipulator to the harvest zone. Both cart propulsion and scissor lift as well as the camera system and manipulator were controlled by the system's main computer. The whole system was powered by 24 V rechargeable batteries.

4.1.1 | End effector design

The end effector is the tool mounted at the last link of the robot arm. The purpose of the end effector in this robot was to facilitate safe removal of the fruit from the plant and also to hold it during transportation to a container.

FIGURE 1 Schematic top and side view of one aisle in a sweet pepper greenhouse. In this situation, each plant in a row of plants has three stems. The growing architecture in the "Y" shape results in a double row of stems per plant row as seen from the aisle. This is also known as the "double row" system. In the "single row system" each plant in the row would have only one single stem [Color figure can be viewed at wileyonlinelibrary.com]

FIGURE 2 Photos of a sweet pepper crop in the greenhouse [Color figure can be viewed at wileyonlinelibrary.com]

FIGURE 3 The SWEEPER prototype consists of a Fanuc LR Mate 200iD robot arm mounted on an automated cart with a scissor lift. The end effector mounted at the tip of the robot arm contains a cutting mechanism, an imaging system, and a fruit catching device. The photo shows the prototype with the side panel opened. CB, controller box power and network; CE, controller box end effector; FC, FANUC robot controller; PA, compressor for pressured air; PC, computer; PW, power inverter [Color figure can be viewed at wileyonlinelibrary.com]

As detailed in Figure 4, the end effector comprises a housing for the RGB-D camera and is fitted with custom made LED lighting fixtures, described in Section 4.2.3. The last joint of the robot arm is connected to this housing by a robot arm mount. Furthermore, on top of the housing, a plant stem fixation mechanism is placed with a vibrating knife configured to cut the fruit peduncle driven by an electrical motor. In the first contact position with the plant stem, the cutting edge of the knife is positioned right above the peduncle of a fruit while it is shielded by the stem fixation mechanism to prevent plant damage by the knife. When the cutting action is initiated, by moving the end effector downwards, the fixation mechanism is lifted, thereby providing the knife room to cut downwards through the peduncle. After the peduncle is cut, the fruit catching device holds the fruit which consists of six metal fingers coated by soft plastic. The fingers are attached to the upper part of the camera housing of the end effector. They are spring-loaded to rotate around their mounting point. This enables the fingers to individually flex backwards if they hit an obstacle
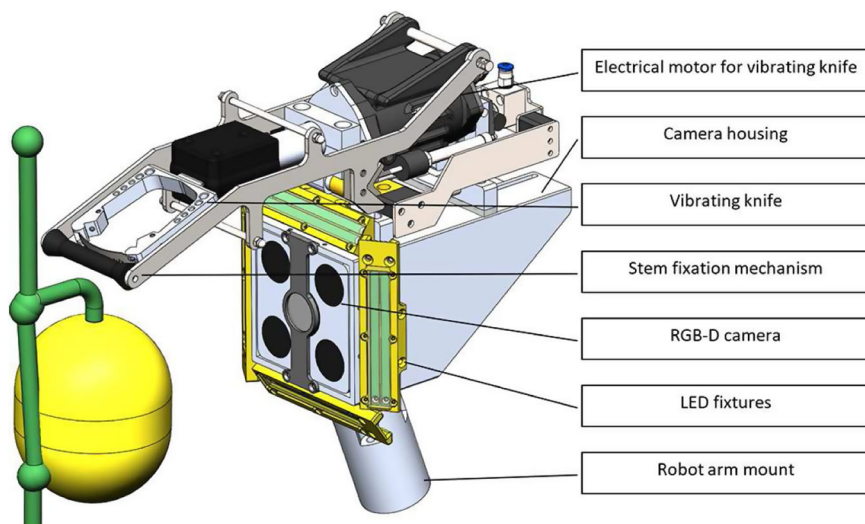
FIGURE 4 End effector components (without catching mechanism). Patent No PCT/NL2019/050396 (pending approval) [Color figure can be viewed at wileyonlinelibrary.com]

FIGURE 5 End effector with cutting device, Fotonic F80 camera, LED illumination, and fruit catching device [Color figure can be viewed at wileyonlinelibrary.com]

while the end effector is approaching the target. Figure 5 shows a photo of the final end effector, including the fingers.

4.2 | Software design

The software developed in the project was crucial to achieve the required functionality. Most software was written in C++ and Python, using ROS Indigo running on Ubuntu 14.04. Most programs were installed on the main computer mounted on the platform. Some functionality, such as image-based obstacle detection, was run on the main computer's GPU to speed up operation.

4.2.1 | Overall operation

The autonomous operation of the robot was defined in a flowchart, describing how sequencing of image-based fruit localization and motion control of platform, robot arm, and end effector was combined to achieve successful harvesting of fruit (see Figure 6). For better readability, some details and most of the error handling are left out in the figure. The basic operation was as follows:

The platform autonomously moves along the plant row and raises itself to the desired working height. The manipulator then moves in a predefined pattern to scan for fruits. As soon as a fruit is detected (see Section 4.2.3), the manipulator moves closer to the fruit, and the location of the stem relative to the fruit is determined (see Section 4.2.4). The end effector is then rotated such that the stem is behind the fruit and then moves towards the fruit using visual servoing. When the fruit is reached, the vibrating knife on the end effector is actuated, and the end effector is moved down to cut the peduncle of the fruit. The fruit is caught in the fingers mounted on the end effector, and the manipulator is moved to the fruit container, where the fruit is dropped. The manipulator is then brought back to where it first saw the fruit, and the scanning procedure and harvesting continue until the scanning pattern is completed. The platform is then lowered to the second harvesting level where harvesting proceeds. When all fruits have been harvested from the current platform position, the platform moves along the rails to the next plant, and the harvesting procedure is repeated. If a fruit harvesting operation fails, a maximum of two additional attempts are made (not shown in flowchart). If the harvesting operation still fails, the fruit is left. When the platform has reached the end of the plant row, it automatically moves back to the starting point of the row.

4.2.2 | High-level control

To execute the flowchart described in the previous section, a state machine-based framework for agricultural and forestry robotics (Hellström & Ringdahl, 2013) was implemented. Each state is usually connected to one or several ROS nodes that perform specific actions such as moving the manipulator or detecting fruits in an image.
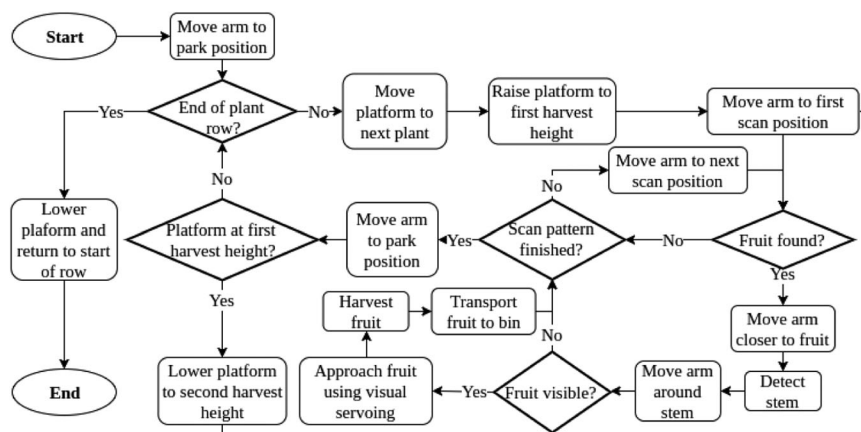
FIGURE 6 A flowchart describing the operation of the final harvesting robot
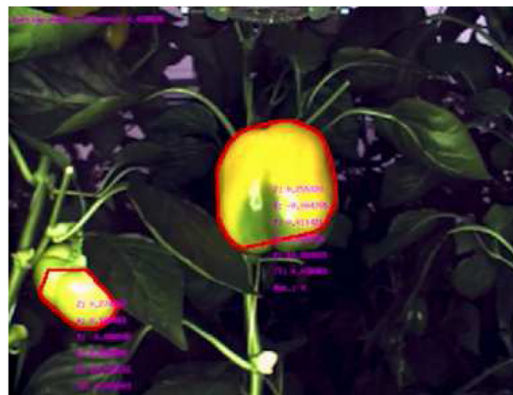
4.2.3 | Fruit detection

A central function in the system is detection of fruits to be harvested. For successful operation, the three-dimensional (3D) location of each fruit must be determined with a high accuracy. The chosen solution is based on an RGB-D camera that simultaneously reports color and depth information. The camera (Fotonic F80; Fotonic Inc., Sweden; Figure 5) employs a time-of-flight technology for depth measurements and uses a single sensor for measuring both RGB and depth, thus allowing fully registered channels. It was proven very robust to varying outdoor illumination conditions with a signal-to-noise ratio well suited for agricultural applications in greenhouses (Ringdahl et al., 2019). Using this camera and a custom built LED-based illumination system, RGB images of the plant were acquired from both overview distance and close range. Since detectability was dependent on the imaging acquisition distance and the sensing system tilt (Hemming, Ruizendaal, Hofstee, & van Henten, 2014; Kurtser & Edan, 2018), a constant tilt upwards of the sensors and illumination rig was applied.

To facilitate high frame-rate operation, a shape and color-based detection algorithm was implemented (Arad et al., 2019). Color constancy is a key factor in the performance of such algorithms and was achieved by applying a filter to obtain homogeneous light distribution in the image. Before operation, the algorithm was calibrated over several sample images (2–3 images), and the user was prompted to select the target fruit. Using this input, color thresholds for detection were automatically set on the basis of the statistics of the selected areas. Calibration needed to be performed only once for each target pepper variety. Several other approaches to automatically determine thresholds were developed and evaluated, see for instance Ostovar, Ringdahl, and Hellström (2018). Once calibrated, the algorithm scanned each acquired image for regions matching the target color thresholds. Detected regions were then further refined by removing detections exceeding predefined minimum/maximum sizes. A *Pepperness* measure *P* was also calculated, for each of the detected peppers according to Equation (1), to further remove misdetections

$$P = \frac{A_P C^2 Z^2}{P_W P_H}, \tag{1}$$

where A_P is the detected area of the pepper in pixels, C is the camera's pixel to cm coefficient, Z is the distance of the pepper (cm), P_W and P_H are standard pepper width and height (controllable parameters in cm). "Holes" in the detected regions were filled using mathematical morphology operations. Finally, depth information from the camera was used to compute the volume of the detected regions. Detected regions were compared with the volume of an average pepper, and the relative size was reported as part of the detection (see Figure 7). This information was then used to further prune false detections, avoid nonharvestable fruit clusters, and define harvest priorities. The exact 3D location of the point of mass was calculated using the depth information extracted from the detected region and a standard procedure of pixel-to-world transformation of the region (e.g., Wei & Ma, 1994; Zhang & Pless,


FIGURE 7 Example of real-time fruit detection. The red curves indicate detected areas [Color figure can be viewed at wileyonlinelibrary.com]

2004). Given the subsets of regions that were classified as peppers to be harvested, a methodology for harvesting sequencing was defined. Several options for harvesting sequencing were reviewed, including optimization of harvesting distance (Edan, Flash, Peiper, Shmulevich, & Sarig, 1991; Zion et al., 2014). The heuristic that was implemented was harvesting in a top-down sequence to facilitate harvesting of clusters, followed by closest to the center to facilitate proper visual servoing that keeps the target in the middle of the image.

4.2.4 | Stem detection

As described in Section 4.2.1, the manipulator rotates around the stem such that the stem is behind the fruit as seen from the camera. To enable this, a method to estimate at what angle the fruit was positioned around the stem was developed. First the images were semantically segmented using a deep learning approach (Barth, IJsselmuiden, Hemming, & Van Henten, 2017, 2018). In this way, the fruit and stem were identified, from which the centers of each plant part could be calculated. Detected stem regions were processed with an Canny edge detector, and the resulting edge image was used to detect straight lines (the estimated path of a stem) by a Hough transform. From the center of the detected stem, a rectangular search region of 200 × 200 pixel was defined for the fruit. The largest connected region inside the search region was selected as fruit region. Around the center of mass of the selected region, the fruit position estimation was refined with a 125 pixel circular mask. The center of mass of the refined region was selected as final fruit center. The corresponding stem center was calculated in the same horizontal plane. Figure 8 illustrates the method applied in unmodified greenhouse conditions.

When the center of the fruit and stem was determined in one viewpoint, the position of the fruit around the stem (angle) could be determined, knowing that the average distance between the fruit center and the stem is 4 cm and the distance of the camera and the fruit surface is 20 cm. However, because this method cannot differentiate if the fruit is in the front or the back of the stem, two
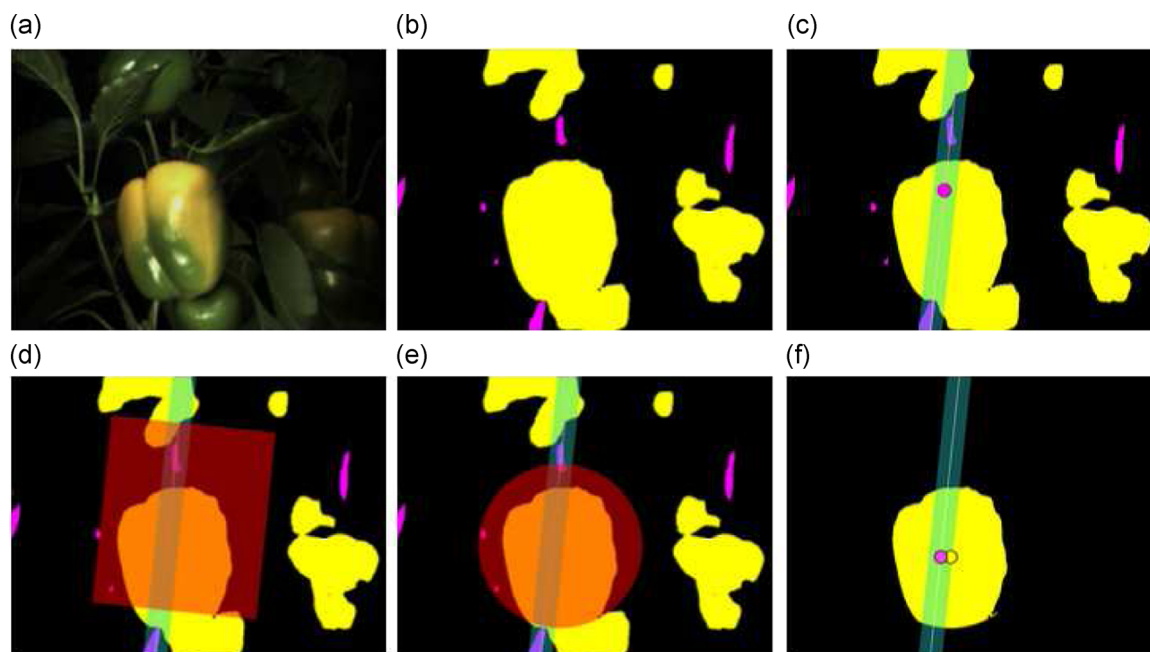
FIGURE 8 Method for estimating fruit and stem centers. (a) Original color image. (b) Semantic segmentation into classes background (black), stems (magenta), and fruit (yellow). (c) Stem pose estimation and found stem center in the image. (d) Search region for fruit within 200 × 200 pixel rectangle; the largest connected region was selected. (e) Around center of mass of selected region, the fruit estimation was refined with a 125 pixel circular mask. (f) Center of mass of refined fruit estimation was selected as final fruit center and corresponding stem center in the horizontal plane as final stem center [Color figure can be viewed at wileyonlinelibrary.com]

viewpoints were required to confirm the proper angle of the fruit. The method was evaluated using 45 greenhouse images for which the ground truth angles between fruit and stem were known. In 73% of the cases, the error was <25°, which was the accuracy requirement set by the mechanical constraints of the end effector (Barth, Hemming, & Van Henten, 2019).

4.2.5 | Motion control

Once a fruit had been detected as described above, the robot arm should move the end effector to a position from which the fruit could be harvested while avoiding obstacles. This is a nontrivial task for several reasons. In general, the robot arm is moved by changing the angles of the six motor-controlled joints in the arm. Finding joint angles for a given goal position is known as the inverse kinematics problem, which in general has several possible solutions. The problem is further complicated by the fact that not only the position, but also the orientation of the end effector must be controlled. To move the end effector along a given path toward the fruit, a sequence of solutions of the inverse kinematics problem has to be computed. Mostly, motion control of the robot arm was implemented using dedicated motion planning software. Several kinds of motion planners and kinematic solvers available in ROS MoveIt! were evaluated, and the lazy PRM* (Bohlin & Kavraki, 2000) planner from the OMPL package and TRAC-IK (Beeson & Ames, 2015) kinematic solver was finally chosen. For the final approach to the fruit, visual servoing was applied, aiming at keeping the detected center of the

fruit in a predetermined position in the camera image. By this procedure, requirements on camera calibration and 3D coordinate estimation were substantially lowered, and the accuracy of end effector positioning increased substantially.

5 | GREENHOUSE TESTING AND PERFORMANCE EVALUATION

The finalized robotic system[6] was evaluated in a commercial sweet pepper production greenhouse in IJsselmuiden, the Netherlands, during June 2018. The procedure for testing and evaluation of results is described in the remaining of this section.

5.1 | Testing procedure

The greenhouse was set up as described in Section 3. Two rows were selected for robotic harvesting experiments, with each comprising 100 stems of the sweet pepper variety Sardinero, followed by 100 stems of the variety Gialte. In this way, the hypothesis that Sardinero would be more suitable for robotic harvesting than Gialte could be tested. The motivation for this hypothesis is that a longer peduncle (fruit stem) should allow more free space to position the end effector

---

[6] A video of the final prototype can be found at http://www.sweeper-robot.eu/videoclips and https://www.youtube.com/watch?v=VbW1ZW8NC2E.

and that a long peduncle should reduce the risk of damaging the fruit by cutting into the fruit body.

As sweet pepper commercially is harvested before the complete fruit body turns from green to yellow, each fruit with at least a 5 cm^2 big yellow colored patch was considered ripe and was manually labeled with a fruit number. Unripe fruits were not labeled and not selected to be harvested by the robot.

Half of the plant stems of both varieties were modified to simulate idealized circumstances, with low occlusion and no clusters interfering with the end effector's reachability. The proposed modifications were introduced after consulting with commercial growers and agronomy experts. The modification was done by removing leafs that occluded a labeled fruit from a frontal perspective. Neighboring fruits that might interfere with a harvest attempt (e.g., clusters) were also removed. Figure 9 illustrates this modification. It was hypothesized that performance for the modified crop would be significantly higher than for the commercial (unmodified) crop.

The current double row growing architecture (as shown in Figure 1) does not allow robotic harvesting from both sides of the stem (front and back) since fruits may be visually and physically occluded by the row of stems. To analyze the potential of the robot in a best fit cropping system (where the robot can reach the stem from both sides), we also calculated the robot performance by only considering fruits that were in front of the row. In the following, this cropping system is referred to as the single row system. For this, only fruits positioned in front of the row (positioned over −90° or +90°) were taken into account. The resulting percentages are with regard to only these fruits.

FIGURE 9 Example of the crop before (left) and after modification (right). The red dotted circles indicate the plant element that have been manually removed [Color figure can be viewed at wileyonlinelibrary.com]

The actual testing procedure started by positioning the robot at the beginning of the plant row with the selected plant stems. The robot was then started to perform the autonomous harvest cycle as described in Section 4.2.1. After the robot finished harvesting fruits from all stems, the remaining ripe fruits that the robot was not able to harvest were manually harvested. In this period of the harvesting season, 4–5 days were the typical period between two consecutive manual harvest actions. Therefore, the robotic harvesting experiment was then paused for 5 days to let the next fruit setting ripen, before starting a new harvest trial at the same plant stems.

5.2 | Performance measures

The harvest cycle consists of a sequence of substeps that all have to work for a fruit to be successfully harvested. To improve understanding and analysis of the test results, success of the following five substeps were logged: fruit detected, fruit reached, fruit cut, fruit caught, and fruit in container.

For each reached fruit, the end effector knife positioning error was measured in two ways (the robot was paused during measurements): the Euclidean distance from the bottom center of the knife of the end effector to the top center of the peduncle (manually determined using a tape measure) and the difference in angle of the end effector with the stem and the angle between the fruit and the stem (manually determined by measuring the difference in angle).

The time spent in the different steps of the harvest cycle was logged. These steps were platform movement, fruit localization, obstacle localization, visual servoing, detach fruit, and put fruit in container (move to storage bin and back).

6 | PERFORMANCE RESULTS

In total, 262 fruits were attempted to be harvested: 104 in the modified crop (66 Sardinero and 38 Gialte) and 159 in the unmodified crop (99 Sardinero and 59 Gialte).

Results for all combinations of growing conditions (pepper variety, single/double row, modified/unmodified) are presented in Table 1, with success rates after each one of the five substeps of the harvesting cycle. Each column contains the fraction of fruits successfully completing the corresponding substep. Hence, success rates for the entire harvesting cycle can be found in the right-most column. Table 2 presents noncumulative success rates for each individual substep for the same data. From this table, bottlenecks can be identified.

For all ripe fruits, percentage of coloration determined manually based on the average ripeness was 69% and 87% for the Sardineroi and Gialtei varieties, respectively.

The most common failure of fruit localization in the unmodified condition was the occlusion of fruit by leaves of the same plant stem or neighboring stems. Occlusions were hardly present in the modified condition.

TABLE 1 Cumulative success rates after each one of the five substeps in the harvesting cycle

	Fruit detected	Fruit reached	Fruit cut	Fruit caught	Fruit in container
Double row					
Modified					
Gialte	97%	92%	84%	71%	71%
Sardinero	68%	61%	47%	36%	36%
All	79%	72%	61%	49%	49%
Commercial					
Gialte	78%	44%	31%	24%	24%
Sardinero	64%	34%	20%	16%	14%
All	69%	38%	24%	19%	18%
Single row					
Modified					
Gialte	97%	91%	91%	81%	81%
Sardinero	74%	63%	51%	43%	43%
All	85%	76%	70%	61%	61%
Commercial					
Gialte	83%	55%	43%	33%	33%
Sardinero	65%	40%	35%	27%	23%
All	73%	47%	38%	30%	29%

In addition, for the unmodified condition, fruit clusters could cause the robot to center in the middle of the cluster, as opposed to the desired middle of the top fruit. The fruit recognition algorithm was sometimes not able to distinguish individual fruit in the clusters. A center error in this phase caused the next phase of the obstacle detection to fail and abort the harvesting attempt. Sometimes, the distance reading of the fruit center was incorrect due to an occluding leaf coming into view during the centering of the robot, causing the robot to abort the current attempt.

When the fruit was properly centered, the obstacle detection took a first overview image to segment the stem and the fruit.

TABLE 2 Noncumulative success rates for each one of the five substeps in the harvesting cycle

	Fruit detected	Fruit reached	Fruit cut	Fruit caught	Fruit in container
Double row					
Modified					
Gialte	97%	95%	91%	85%	100%
Sardinero	68%	90%	77%	77%	100%
All	79%	91%	85%	80%	100%
Commercial					
Gialte	78%	56%	70%	77%	100%
Sardinero	64%	53%	59%	80%	88%
All	69%	55%	63%	79%	95%
Single row					
Modified					
Gialte	97%	94%	100%	89%	100%
Sardinero	74%	85%	81%	84%	100%
All	85%	89%	92%	87%	100%
Commercial					
Gialte	83%	66%	78%	77%	100%
Sardinero	65%	62%	88%	77%	85%
All	73%	64%	81%	79%	97%

Sometimes this failed because the situation was so unique, and it was not covered in the training data of the machine learning algorithm. Sometimes only one of the two classes was detected, causing a failure of this action.
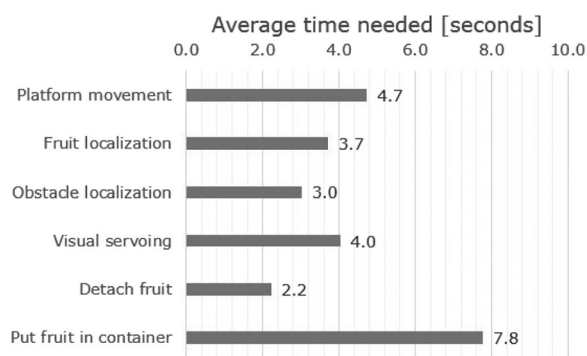
Most failures during visual servo control were due to losing sight of the fruit, notably from leaves coming into the view when the end effector moved closer by. This most often happened in the last 5–10 cm to the fruit. For the modified condition, failures during visual servo control were rare. Visual servo control could also fail when the end effector pushed away the fruit (getting in contact with the stem or a neighboring fruit). In the current mechanical design, the fingers to catch fruit sometimes push the plant away while the end effector is approaching the fruit. This is because the fingers, even constructed to do so, do not flex away easy enough when touching leaves or other fruits in the way. The target fruit then never comes closer to the tool center point, aborting the procedure when the manipulator reached the boundary of its workspace.

Detachment of the fruit could fail in multiple ways. First, the end effector might have not been positioned accurately regarding the angle of the end effector and the fruit and stem (i.e., not in line with each other), but also regarding the Euclidean distance of the knife and the peduncle, which could be too much after visual servo control. In such cases, the knife failed to intersect with the peduncle fully, causing only a partial or no cut of the fruit. Second, it was observed that the knife was sometimes slipping off the peduncle, especially with the Sardinero variety with its longer and more vertical peduncles. Third, the motion downward of the end effector was not always possible because the manipulator could already be near the end of its workspace when the knife was was positioned on top of the peduncle after visual servo control.

When the fruit was cut, it was required to be caught by the catching device. On a rare occasion, this failed because the fruit bounced just on the edge of the device. In some other rare occasions, the fruit got entangled in side branches or leaves while falling down after cutting, causing not to end up in the catching device.

The total average cycle time was 24 s (ranging between 18 and 25 s). It is important to mention that, due to safety reasons, the robot was not operated at the maximum speed technically possible. This was to protect the researchers working close to the system to collect data and also to protect the mechanical components of the robot. The unique end effector and the camera might otherwise have been easily damaged by unexpected self-collisions or collisions with the crop or greenhouse equipment. Laboratory experiments with the same prototype showed that it is possible to harvest one fruit in <15 s (excluding platform movements) Figure 10.

The measured positioning error of the end effector after visual servoing control and before the cutting operation gives information on the combined accuracy of fruit localization, stem–fruit angle estimation, and visual servoing control. Figure 11 shows average errors for combinations of modified/unmodified conditions and crop varieties, computed for the simulated single row system. For both crop varieties, the unmodified, commercial crop condition results in larger error, measured by both distance and angle.

Average time needed [seconds]

Platform movement 4.7
Fruit localization 3.7
Obstacle localization 3.0
Visual servoing 4.0
Detach fruit 2.2
Put fruit in container 7.8

FIGURE 10 Average time needed for the different robot subtasks

7 | DISCUSSION

Results show large differences between a modified and unmodified crop. Under a single row system assumption, harvest performance averaged over both crop varieties was 61% for the modified crop as opposed to 29% of the unmodified crop. Broken down into the subtasks fruit detected, fruit reached, fruit cut, fruit caught, and fruit put in container, the difference in performance was 12%, 29%, 32%, 31%, and 32%, respectively. This difference can solely be explained by the removal of leaves and neighboring fruit. Regarding the former, leaves occlude the computer vision in many stages of the harvest cycle, causing early aborts. Regarding the latter, neighboring fruit can interfere with the end effector's motion to position the tool accurately. Neighboring fruit can also affect the fruit localization process.

The results indicate that the performance of the robot could be increased by addressing occlusions and clusters of fruit. Approaches like plant breeding, mechanical solutions, or growing architecture, and crop maintained strategies could help to achieve this.

The hypothesis that the Sardinero crop variety would be more suitable for robotic harvesting compared with the Gialte variety could not be confirmed. It turned out that the longer and more vertical peduncles of Sardinero resulted in a less stable contact point for the knife such that sometimes the knife did not cut through but slipped off the peduncle. Furthermore, the longer peduncles increased the uncertainty about the exact location of the cutting point as the developed system only locates the fruit body and not the
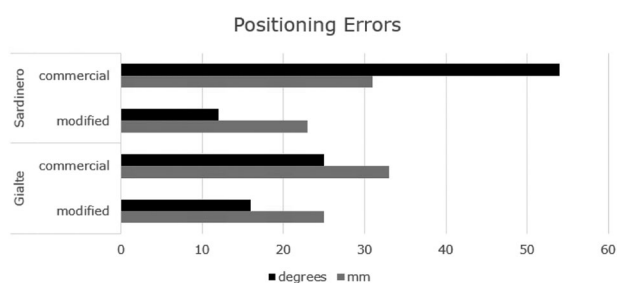
cutting point itself. This is also reflected by the observed higher end effector positioning errors for Sardinero, as shown in Figure 11. The hypothesis that a longer peduncle should reduce the risk of cutting into fruit body was not confirmed. As the fruit immediately drops down into the catching fingers once the peduncle is cut, typically no fruit damage occurs, even when the robot continues a bit more with the downwards cutting motion. This emphasizes the need for experimentation in real-world conditions.

Under a single row system assumption, the harvest success rate for the modified condition was 81% for Gialte and 43% for Sardinero. For the unmodified condition, results were closer at 36% for Gialte and 23% for Sardinero. The results also show that the fruit detection rate for the variety Gialte was higher than for Sardinero for all scenarios. The higher average degree of ripeness of the fruits of the Gialte variety (as described in Section 6) may have facilitated the detection and correct localization of the target fruits. The fruit ripeness is, however, not a characteristic of the variety but changes over time. It should be noted that the reported experiment only included two varieties. It was also observed that during the 4 weeks the experiments took place, the crop conditions/crop geometry like openness of the crop and appearance of fruit clusters changed a lot within the same variety. These changes seemed even larger than the difference between the two varieties. The different performance for different crop varieties should be further researched, ideally in cooperation with breeders. It is suggested to develop a robust evaluation method to simplify performance measurements of robotic harvesting. This would speed up the overall design process of an improved robotic system.

The results show that a modified cropping system significantly increases harvest performance. Further development should therefore concentrate on usage in modified cropping systems, such as the previously described single row system. Such modifications should not negatively influence plant growth or yield and should always be acceptable to the commercial growers. In general, the estimated harvest performance, on average 29% in the unmodified crop and 61% in the modified crop, shows promise for an autonomous preharvest of the crop, whilst the remainder would be harvested by humans. Compared with previous results from the CROPS project (Bac et al., 2017; Bontsema et al., 2014) 6% for unmodified and 26% for modified crops, performance has increased significantly. Comparable improvements have been made to the cycle time, currently at an average of 24 s, compared with 94 s for CROPS and 35–40 s by Harvey (Lehnert et al., 2017) not including platform movement. Additional evaluation should also be conducted in different seasons and greenhouses to ensure robustness.

Positioning Errors

Sardinero commercial
Sardinero modified
Gialte commercial
Gialte modified

0 10 20 30 40 50 60

■ degrees ■ mm

FIGURE 11 Average positioning errors of the end effector after visual servoing control and before the cutting operation for the different crop varieties and cropping systems

8 | SUGGESTED IMPROVEMENTS

The field tests provided valuable insights in the performance of the integrated system and how its modules functioned together. The following bottlenecks and possible improvements have been identified:

Ways to increase performance of the submodules for detection, reaching, cutting, and catching should be further investigated.

The performance results and failure analysis indicate that a different type of robot arm with an increased workspace and/or different mounting pose may improve the success rate. Compared with the overall size of the platform, the robotic arm (and its workspace) is rather small. However, an arm with longer joints will most likely also have more difficulties to plan and execute a collision free motion in this dense environment. An arm with more DOF will increase the computational efforts to plan the trajectory.

A smaller end effector would increase reachability and would decrease the risk of collisions with the crop. The end effector size can be reduced by using a smaller camera, light unit, or catching device.

As described above, the fingers of the catching device do not flex away enough when touching leaves or other fruits, thereby preventing in some occasions fruits from being reached and harvested. A redesign of the catching device is therefore recommended.

Transportation of the fruit to the storage bin currently consumes a lot of time compared with the other actions. The speed of the manipulator should be increased or alternative ways of storing the fruit should be considered.

Another insight concerns error handling and uncertainty control. Currently, when the robot loses sight of the fruit or cannot reach a certain position, harvesting is simply aborted. Instead, the system should try to recover by backtracking to a point from which the operation can be resumed.

9 | CONCLUSIONS

The developed prototype was able to fully autonomously harvest sweet pepper fruits in a commercial greenhouse. For the current commercial cropping system (double row), 18% of all ripe fruits were harvested in the commercial crop and 49% in the modified crop. For this modification, most occluding leaves and fruit clusters have to been pruned away beforehand. For the (simulated) single row plant system, 29% of all ripe fruits were harvested in the commercial crop and 61% in the modified crop. The average cycle time to harvest a fruit was 24 s. The robot fulfils three of the four defined requirements for operations in commercial greenhouses (Section 3); the interface with other AGVs was not addressed in the prototype. The hypothesis regarding the positive effect of crop modification was confirmed. This shows that breeding or other ways to enhance fruit visibility or decrease fruit clustering have great potential in the future of robotic harvesting.

ACKNOWLEDGMENTS

ORCID

Boaz Arad http://orcid.org/0000-0003-0855-1387
Jos Balendonck http://orcid.org/0000-0002-6949-6409
Ruud Barth http://orcid.org/0000-0002-9216-1607
Ohad Ben-Shahar http://orcid.org/0000-0001-5346-152X
Yael Edan http://orcid.org/0000-0002-7430-8468
Thomas Hellström http://orcid.org/0000-0001-7242-2200
Jochen Hemming http://orcid.org/0000-0002-3805-6160
Polina Kurtser http://orcid.org/0000-0003-4685-379X
Ola Ringdahl http://orcid.org/0000-0002-4600-8652

REFERENCES

Adamides, G., Katsanos, C., Constantinou, I., Christou, G., Xenos, M., Hadzilacos, T., & Edan, Y. (2017). Design and development of a semi-autonomous agricultural vineyard sprayer: Human–robot interaction aspects. *Journal of Field Robotics*, 34, 1407–1426. https://doi.org/10.1002/rob.21721

Almendral, K. A. M., Babaran, R. M. G., Carzon, B. J. C., Cu, K. P. K., Lalanto, J. M., & Abad, A. C. (2018). Autonomous fruit harvester with machine vision. *Journal of Telecommunication, Electronic and Computer Engineering*, 10, 79–86.

Arad, B., Kurtser, P., Ehud, B., Harel, B., Edan, Y., & Ben-Shahar, O. (2019). Controlled lighting and illumination-independent target detection for real-time cost-efficient applications. The case study of sweet pepper harvesting robots. *Sensors*, 19(6), 1390.

Bac, C. W., Hemming, J., van Tuijl, B., Barth, R., Wais, E., & van Henten, E. J. (2017). Performance evaluation of a harvesting robot for sweet pepper. *Journal of Field Robotics*, 34, 1123–1139. https://doi.org/10.1002/rob.21709

Bac, C. W., van Henten, E. J., Hemming, J., & Edan, Y. (2014). Harvesting robots for high-value crops: State-of-the-art review and challenges ahead. *Journal of Field Robotics*, 31, 888–911.

Barth, R., Hemming, J., & van Henten, E. (2019). Angle estimation between plant parts for grasp optimisation in harvest robots. *Biosystems Engineering*, 183, 26–46. https://doi.org/10.1016/j.biosystemseng.2019.04.006

Barth, R., Hemming, J., & van Henten, E. J. (2016). Design of an eye-in-hand sensing and servo control framework for harvesting robotics in dense vegetation. *Biosystems Engineering*, 146, 71–84. https://doi.org/10.1016/j.biosystemseng.2015.12.001

Barth, R., IJsselmuiden, J., Hemming, J., & van Henten, E. J. (2017). Synthetic bootstrapping of convolutional neural networks for semantic plant part segmentation. *Computers and Electronics in Agriculture*, https://doi.org/10.1016/j.compag.2017.11.040

Barth, R., IJsselmuiden, J., Hemming, J., & van Henten, E. J. (2018). Data synthesis methods for semantic segmentation in agriculture: A *capsicum annuum* dataset. *Computers and Electronics in Agriculture*, 144, 284–296. https://doi.org/10.1016/j.compag.2017.12.001

Baxter, P., Cielniak, G., Hanheide, M., & From, P. (2018). *Safe human-Robot interaction in agriculture*. Paper presented at the Companion of the 2018 ACM/IEEE International Conference on Human-Robot Interaction, Chicago, IL, 59–60.

Bechar, A., & Vigneault, C. (2017). Agricultural robots for field operations. part 2: Operations and systems. *Biosystems Engineering*, 153, 110–128.

Beeson, P., & Ames, B. (2015). *Trac-ik: An open-source library for improved solving of generic inverse kinematics*. 2015 IEEE-RAS 15th International

Conference on Humanoid Robots (Humanoids), 928-935. https://doi.org/10.1109/HUMANOIDS.2015.7363472

Berenstein, R., & Edan, Y. (2018). Automatic adjustable spraying device for site-specific agricultural application. *IEEE Transactions on Automation Science and Engineering*, 15, 641–650.

Blackmore, S. (2016). *Towards robotic agriculture. Autonomous Air and Ground Sensing Systems for Agricultural Optimization and Phenotyping.* International Society for Optics and Photonics, volume 9866, 986603.

Bohlin, R., & Kavraki, L. E. (2000). *Path planning using lazy prm.* Proceedings 2000 ICRA. Millennium Conference. IEEE International Conference on Robotics and Automation. Symposia Proceedings (Cat. No. 00CH37065), volume 1, 521-528. https://doi.org/10.1109/ROBOT.2000.844107

Bontsema, J., Hemming, J., Pekkeriet, E., Saeys, W., Edan, Y., Shapiro, A., & Ringdajl, O. (2014). Crops: High tech agricultural robots. International Conference of Agricultural Engineering AgEng 2014, The European Society of Agricultural Engineers, 1-8.

Botterill, T., Paulin, S., Green, R., Williams, S., Lin, J., Saxton, V., & Corbett-Davies, S. (2017). A robot system for pruning grape vines. *Journal of Field Robotics*, 34, 1100–1122.

Bulanon, D. M., & Kataoka, T. (2010). Fruit detection system and an end effector for robotic harvesting of fuji apples. *Agricultural Engineering International: CIGR Journal*, 12, 203–210.

Ceres, R., Pons, J., Jimenez, A., Martin, J., & Calderon, L. (1998). Design and implementation of an aided fruit-harvesting robot (agribot). *Industrial Robot: An International Journal*, 25, 337–346.

Comba, L., Gay, P., Piccarolo, P., & Ricauda Aimonino, D. (2010). *Robotics and automation for crop management: Trends and perspective.* International Conference Ragusa SHWA2010, 471-478.

De-An, Z., Jidong, L., Wei, J., Ying, Z., & Yu, C. (2011). Design and control of an apple harvesting robot. *Biosystems Engineering*, 110, 112–122.

Duckett, T., Pearson, S., Blackmore, S., Grieve, B., & Smith, M. (2018). White paper-agricultural robotics: The future of robotic agriculture. Retrieved from https://uwe-repository.worktribe.com/output/866226

Edan, Y., Flash, T., Peiper, U. M., Shmulevich, I., & Sarig, Y. (1991). Near-minimum-time task planning for fruit-picking robots. *IEEE Transactions on Robotics and Automation*, 7, 48–56.

Edan, Y., Han, S., & Kondo, N. (2009). Automation in agriculture. In S. Nof (Ed.), *Springer handbook of automation* (pp. 1095–1128). Berlin, Heidelberg: Springer.

Edan, Y., & Miles, G. E. (1993). Design of an agricultural robot for harvesting melons. *Transactions of the ASAE*, 36, 593–603.

Edan, Y., & Miles, G. E. (1994). Systems engineering of agricultural robot design. *IEEE Transactions on Systems, Man, and Cybernetics*, 24, 1259–1265.

Edan, Y., Rogozin, V., Flash, T., & Miles, G. E. (2000). Robotic melon harvesting. *IEEE Transactions on Robotics and Automation*, 16, 831–834.

Eizicovits, D., & Berman, S. (2014). Efficient sensory-grounded grasp pose quality mapping for gripper design and online grasp planning. *Robotics and Autonomous Systems*, 62, 1208–1219. https://doi.org/10.1016/j.robot.2014.03.011

Eizicovits, D., van Tuijl, B., Berman, S., & Edan, Y. (2016). Integration of perception capabilities in gripper design using graspability maps. *Biosystems Engineering*, 146, 98–113. https://doi.org/10.1016/j.biosystemseng.2015.12.016

Feng, Q., Zou, W., Fan, P., Zhang, C., & Wang, X. (2018). Design and test of robotic harvesting system for cherry tomato. *International Journal of Agricultural and Biological Engineering*, 11, 96–100.

Ferreira, M. D., Sanchez, A. C., Braunbeck, O. A., & Santos, E. A. (2018). Harvesting fruits using a mobile platform: A case study applied to citrus. *Engenharia Agrícola*, 38, 293–299.

Foglia, M. M., & Reina, G. (2006). Agricultural robot for radicchio harvesting. *Journal of Field Robotics*, 23, 363–377.

Halstead, M., McCool, C., Denman, S., Perez, T., & Fookes, C. (2018). Fruit quantity and ripeness estimation using a robotic vision system. *IEEE Robotics and Automation Letters*, 3, 2995–3002.

Hayashi, S., Ganno, K., Ishii, Y., & Tanaka, I. (2002). Robotic harvesting system for eggplants. *Japan Agricultural Research Quarterly*, 36, 163–168.

Hayashi, S., Shigematsu, K., Yamamoto, S., Kobayashi, K., Kohno, Y., Kamata, J., & Kurita, M. (2010). Evaluation of a strawberry-harvesting robot in a field test. *Biosystems Engineering*, 105, 160–171.

Hellström, T., & Ringdahl, O. (2013). A software framework for agricultural and forestry robots. *Industrial Robot: An International Journal*, 40, 20–26. https://doi.org/10.1108/01439911311294228

Hemming, J., Ruizendaal, J., Hofstee, J. W., & van Henten, E. J. (2014). Fruit detectability analysis for different camera positions in sweet-pepper. *Sensors*, 14, 6032–6044.

van Henten, E. J., Bac, C., Hemming, J., & Edan, Y. (2013). Robotics in protected cultivation. *IFAC Proceedings Volumes*, 46, 170–177.

van Henten, E., Hemming, J., van Tuijl, B., Kornet, J., Meuleman, J., Bontsema, J., & van Os, E. (2002). An autonomous robot for harvesting cucumbers in greenhouses. *Autonomous Robots*, 13, 241–258.

van Henten, E., van Tuijl, B., Hemming, J., Kornet, J., Bontsema, J., & van Os, E. (2003). Field test of an autonomous cucumber picking robot. *Biosystems Engineering*, 86, 305–313.

Kamilaris, A., & Prenafeta-Boldú, F. X. (2018). Deep learning in agriculture: A survey. *Computers and Electronics in Agriculture*, 147, 70–90.

Kapach, K., Barnea, E., Mairon, R., Edan, Y., & Ben-Shahar, O. (2012). Computer vision for fruit harvesting robots–state of the art and challenges ahead. *International Journal of Computational Vision and Robotics*, 3, 4–34.

Korthals, T., Kragh, M., Christiansen, P., Karstoft, H., Jørgensen, R. N., & Rückert, U. (2018). Multi-modal detection and mapping of static and dynamic obstacles in agriculture for process evaluation. *Frontiers in Robotics and AI*, 5, 28.

Kurtser, P., & Edan, Y. (2018). Statistical models for fruit detectability: Spatial and temporal analyses of sweet peppers. *Biosystems Engineering*, 171, 272–289. https://doi.org/10.1016/j.biosystemseng.2018.04.017

Kurtser, P., & Edan, Y. (2019). Planning the sequence of tasks for harvesting robots. *Submitted.*

Lehnert, C. F., English, A., McCool, C., Tow, A. W., & Perez, T. (2017). Autonomous sweet pepper harvesting for protected cropping systems. *IEEE Robotics and Automation Letters*, 2, 872–879.

Li, K., & Qi, Y. (2018). *Motion planning of robot manipulator for cucumber picking.* 2018 3rd International Conference on Robotics and Automation Engineering (ICRAE), IEEE, 50-54.

Liu, P., ElGeneidy, K., Pearson, S., Huda, M. N., & Neumann, G. (2018). *Towards real-time robotic motion planning for grasping in cluttered and uncertain environments.* Towards Autonomous Robotic Systems: 19th Annual Conference, TAROS 2018, Bristol, UK July 25-27, 2018, Proceedings, volume 10965, Springer, 481.

Ostovar, A., Ringdahl, O., & Hellström, T. (2018). Adaptive image thresholding of yellow peppers for a harvesting robot. *Robotics*, 7, 1–16.

Ringdahl, O., Kurtser, P., & Edan, Y. (2019). Performance of RGB-D camera for different object types in greenhouse conditions. *European Conference on Mobile Robots (ECMR)*, Prague, Czech Republic, 103, 1–6. https://doi.org/10.1109/ECMR.2019.8870935

Ringdahl, O., Kurtser, P., & Edan, Y. (2019). Evaluation of approach strategies for harvesting robots: Case study of sweet pepper harvesting. *Journal of Intelligent & Robotic Systems*, 95(1), 149–164. https://doi.org/10.1007/s10846-018-0892-7

Rodríguez, F., Moreno, J., Sánchez, J., & Berenguel, M. (2013). Grasping in agriculture: State-of-the-art and main characteristics, *Grasping in robotics* (pp. 385–409). London, UK: Springer.

Shamshiri, R. R., Hameed, I. A., Pitonakova, L., Weltzien, C., Balasundram, S. K., Yule, I. J., & Chowdhary, G. (2018). Simulation software and virtual environments for acceleration of agricultural robotics: Features highlights and performance comparison. *International Journal of Agricultural and Biological Engineering*, 11, 15–31.

Silwal, A., Davidson, J. R., Karkee, M., Mo, C., Zhang, Q., & Lewis, K. (2017). Design, integration, and field evaluation of a robotic apple harvester. *Journal of Field Robotics*, 34, 1140–1159.

Tanigaki, K., Fujiura, T., Akase, A., & Imagawa, J. (2008). Cherry-harvesting robot. *Computers and Electronics in Agriculture*, *63*, 65–72.

Tian, G., Zhou, J., & Gu, B. (2018). Slipping detection and control in gripping fruits and vegetables for agricultural robot. *International Journal of Agricultural and Biological Engineering*, *11*, 45–51.

Vitzrabin, E., & Edan, Y. (2016a). Adaptive thresholding with fusion using a RGBD sensor for red sweet-pepper detection. *Biosystems Engineering*, *146*, 45–56.

Vitzrabin, E., & Edan, Y. (2016b). Changing task objectives for improved sweet pepper detection for robotic harvesting. *IEEE Robotics and Automation Letters*, *1*, 578–584.

Wang, H., Hohimer, C. J., Bhusal, S., Karkee, M., Mo, C., & Miller, J. H. (2018). Simulation as a tool in designing and evaluating a robotic apple harvesting system. *IFAC-PapersOnLine*, *51*, 135–140.

Wei, G.-Q., & Ma, S. D. (1994). Implicit and explicit camera calibration: Theory and experiments. *IEEE Transactions on Pattern Analysis and Machine Intelligence*, *16*, 469–480. https://doi.org/10.1109/34.291450

Yuan, S., Lei, Y., Xin, S., & Bing, L. (2016). Design and experiment of intelligent mobile apple picking robot. *Journal of Agricultural Mechanization Research*, *1*, 035.

Zemmour, E., Kurtser, P., & Edan, Y. (2019). Automatic parameter tuning for adaptive thresholding in fruit detection. *Sensors*, *19*, 2130.

Zhang, Q., & Pless, R. (2004). *Extrinsic calibration of a camera and laser range finder (improves camera calibration)*. Intelligent Robots and Systems (IROS). Proceedings. IEEE/RSJ International Conference on, volume 3, IEEE, 2301-2306.

Zhao, Y., Gong, L., Huang, Y., & Liu, C. (2016). A review of key techniques of vision-based control for harvesting robot. *Computers and Electronics in Agriculture*, *127*, 311–323.

Zion, B., Mann, M., Levin, D., Shilo, A., Rubinstein, D., & Shmulevich, I. (2014). Harvest-order planning for a multiarm robotic harvester. *Computers and Electronics in Agriculture*, *103*, 75–81.